Powering an Inorganic Nanodevice with a Biomolecular Motor

by Ricky K. Soong, George D. Bachand, Hercules P. Neves, Anatoli G. Olkhovets, Harold G. Craighead, and Carlo D. Montemagno

Science
Volume 290(5496):1555-1558
November 24, 2000

ATP synthase is an enzyme that creates the energy storage molecule adenosine triphosphate (ATP). ATP is the most commonly used "energy currency" of cells for most organisms. It is formed from adenosine diphosphate (ADP) and inorganic phosphate (Pi). The overall reaction catalyzed by ATP synthase is:

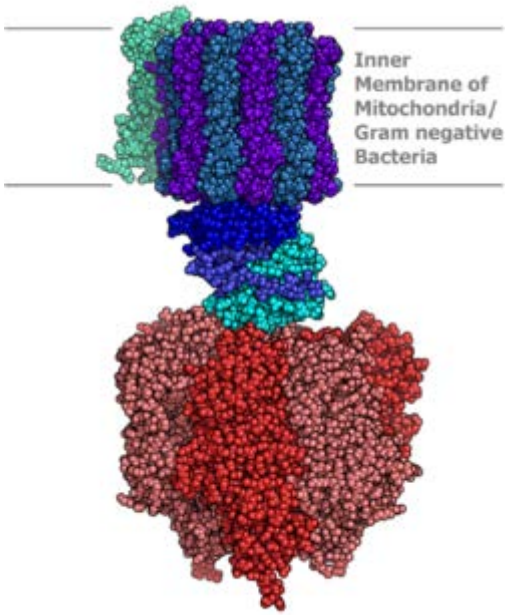

$ADP + Pi + H^+_{out} \rightleftharpoons ATP + H_2O + H^+_{in}$

The formation of ATP from ADP and Pi is energetically unfavorable and would normally proceed in the reverse direction. In order to drive this reaction forward, ATPase couples ATP synthesis during cellular respiration to an electrochemical gradient created by the difference in proton (H+) concentration across the mitochondrial membrane in eukaryotes or the plasma membrane in bacteria. During photosynthesis in plants, ATP is synthesized by ATPase using a proton gradient created in the thylakoid lumen through the thylakoid membrane and into the chloroplast stroma.

ATP synthase consists of two main subunits, FO and F1, **which has a rotational motor mechanism allowing for ATP production**. **Because of its rotating subunit ATP Synthase is a molecular machine**.

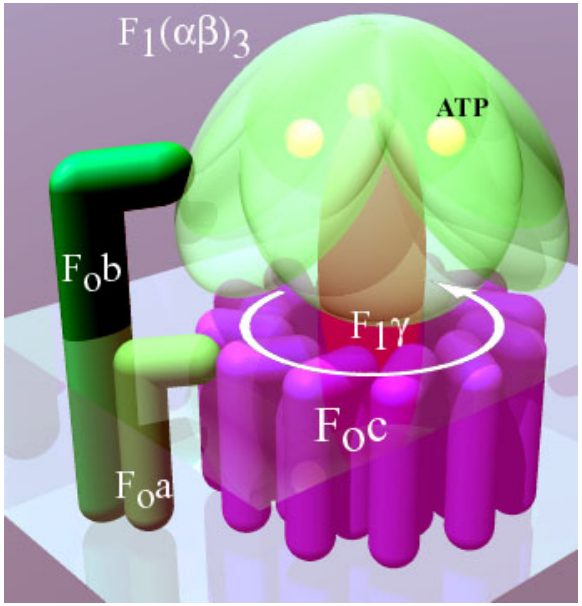

Figure 1 Schematic diagram of the F1-ATPase biomolecular motor–powered nanomechanical device.

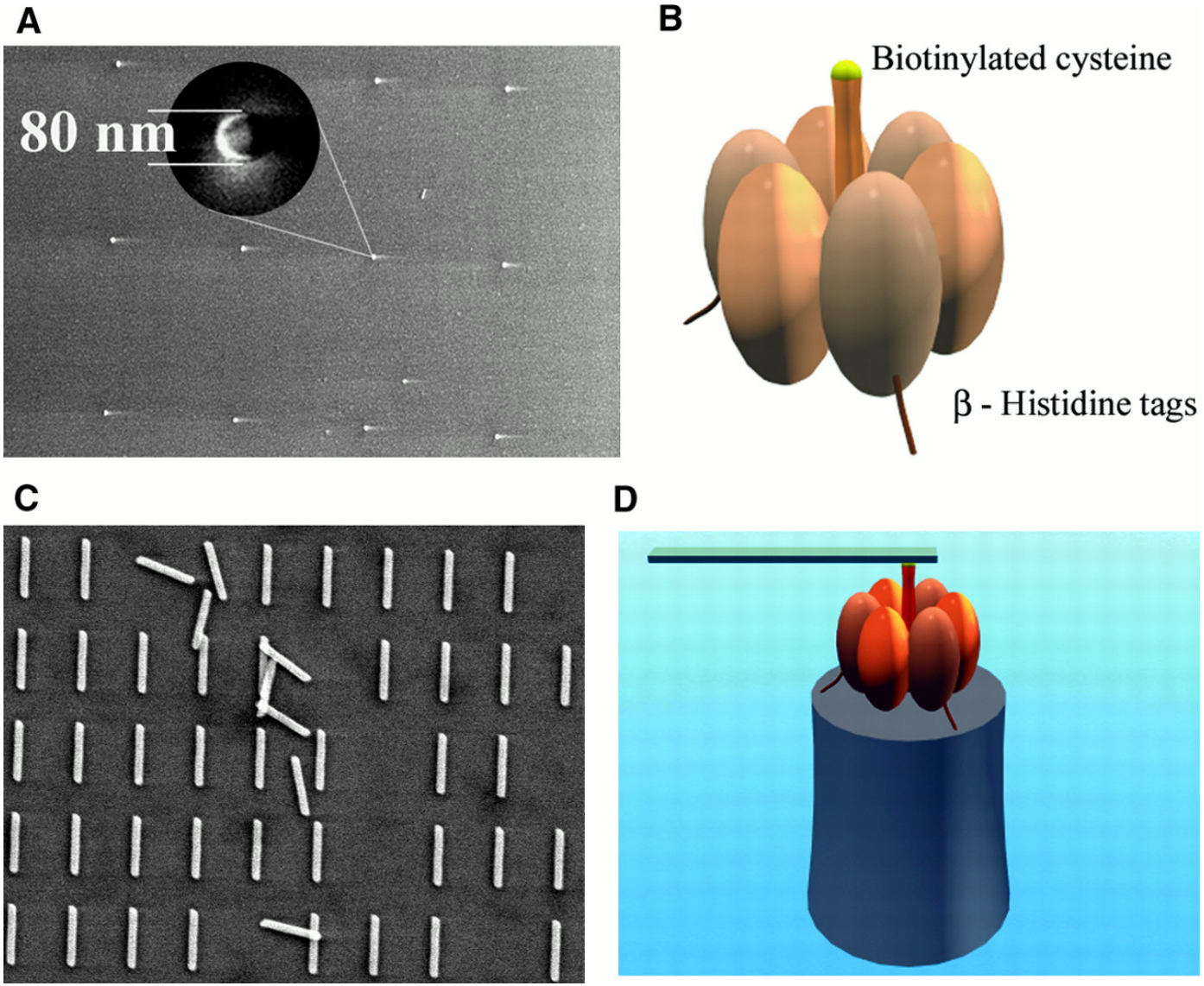

Biotin maleimide

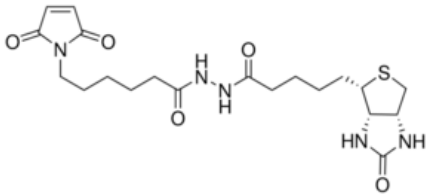

Ricky K. Soong et al. Science 2000;290:1555-1558

Figure 2 Image sequence (viewed left to right) of nanopropellers being rotated anticlockwise at 8.3 rps (A) and 7.7 rps (B) by the F1-ATPase biomolecular motor.

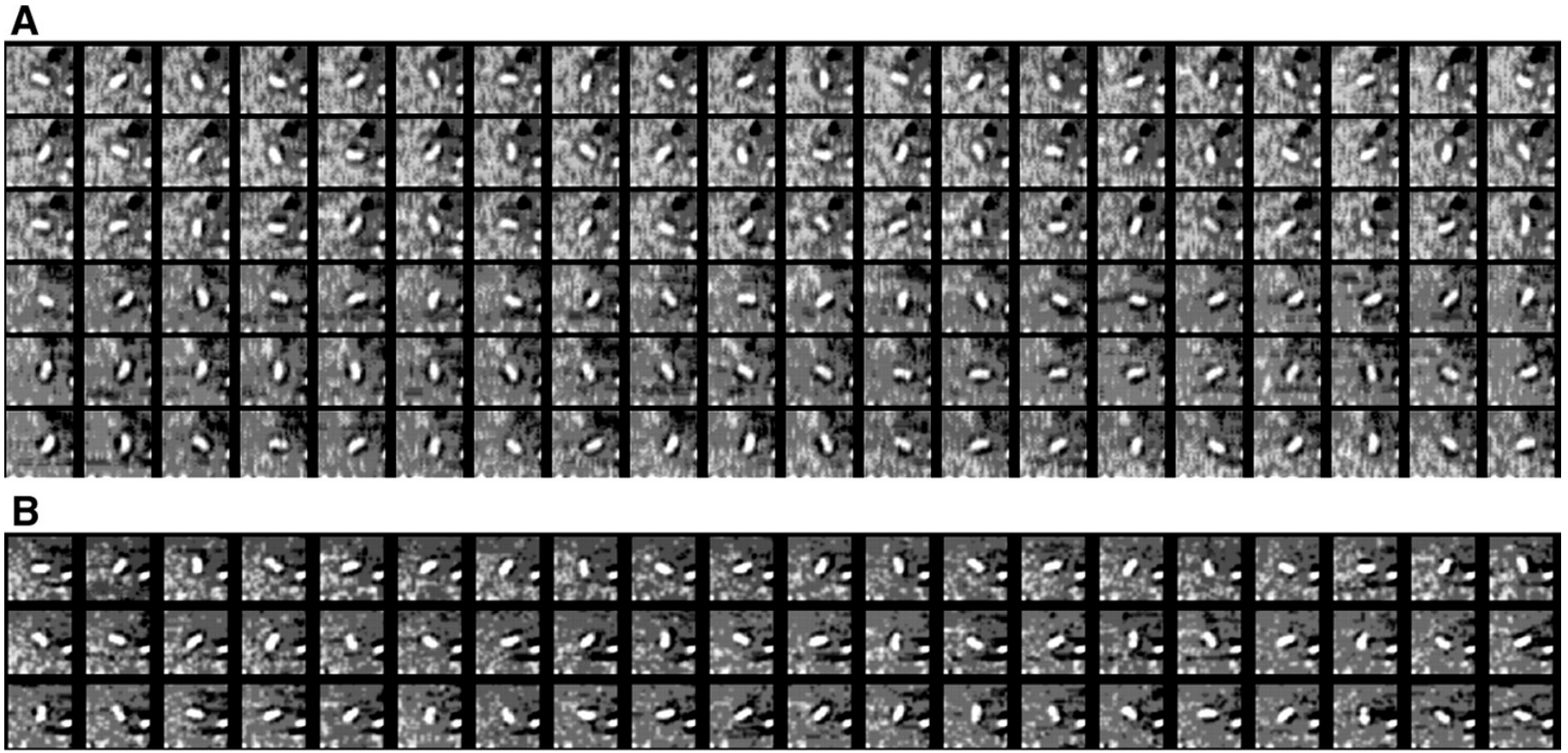

Ricky K. Soong et al. Science 2000;290:1555-1558

Figure 3 Time course of F1-ATPase γ subunit rotation.

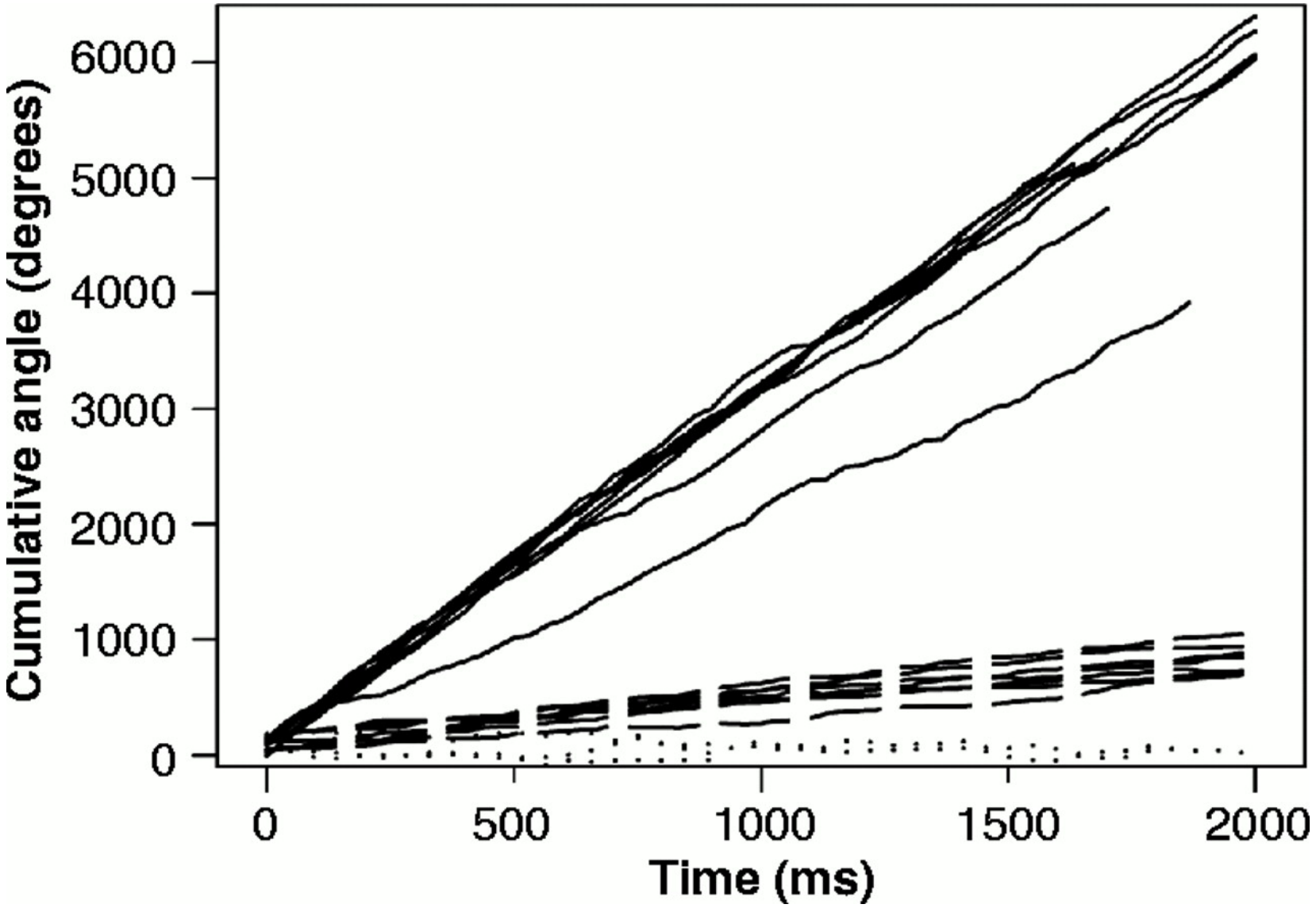

Ricky K. Soong et al. Science 2000;290:1555-1558

Direct observation of the rotation of F_1-ATPase

Hiroyuki Noji*, Ryohei Yasuda†, Masasuke Yoshida* & Kazuhiko Kinosita Jr†

* *Research Laboratory of Resources Utilization, Tokyo Institute of Technology, Nagatsuta 4259, Midori-ku, Yokohama 226, Japan*

† *Department of Physics, Faculty of Science and Technology, Keio University, Hiyoshi 3-14-1, Kohoku-ku, Yokohama 223, Japan*

NATURE | VOL 386 | 20 MARCH 1997

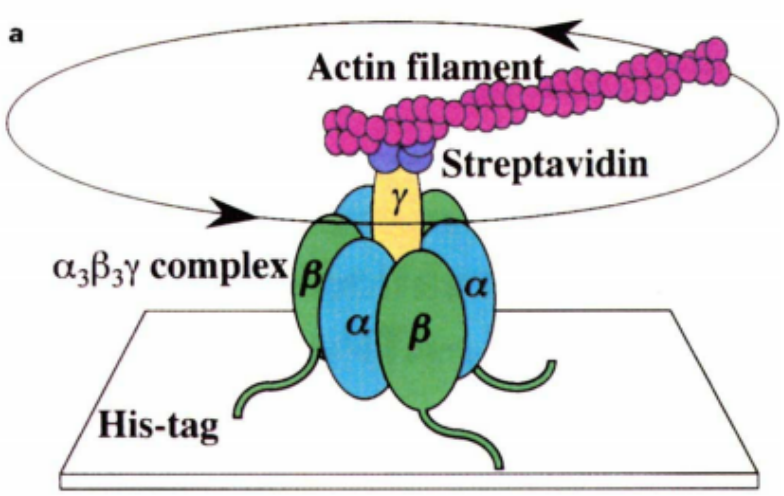

Figure 1 a, The system used for observation of the rotation of the γ-subunit in the $\alpha_3\beta_3\gamma$ subcomplex. **b**, Crystal structure of mitochondrial F_1-ATPase[8] viewed from the membrane side, or from above the glass plate in **a**. Only a part of the structure near the nucleotide-binding site is shown. The observed direction of the rotation of the γ-subunit is indicated by an arrow.

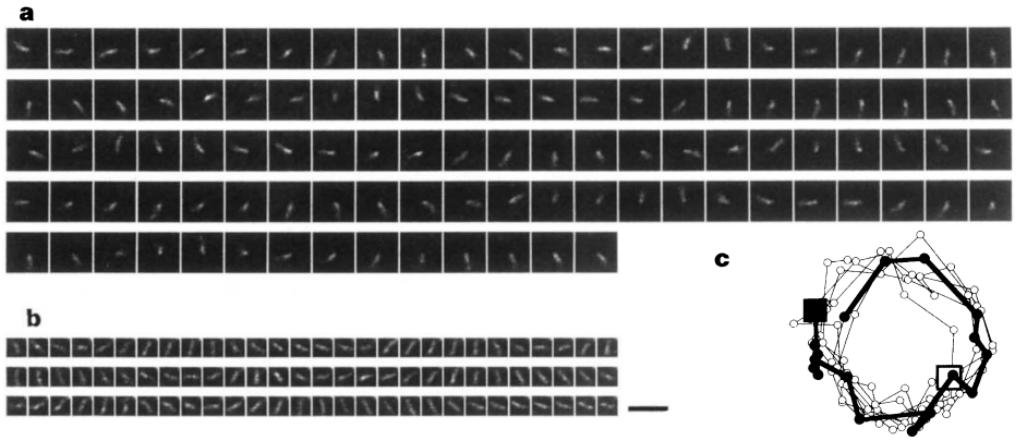

Figure 2 Sequential images of a rotating actin filament attached to the γ-subunit in the $\alpha_3\beta_3\gamma$ subcomplex. In the inverted microscope, the specimen is viewed from the bottom and its mirror image is formed on the camera[23]. Therefore, images shown here correspond to the view from the top (Fig. 1a). **a**, A rotating filament with the rotation axis at one edge. Length from the axis to tip, 2.6 μm; rotary rate, 0.5 r.p.s.; time interval between images, 133 ms. **b**, A rotating filament with the rotation axis at the middle of the filament. Total length of the filament, 2.4 μm; rotary rate, 1.3 r.p.s.; time interval between images, 33 ms. Scale bar, 5 μm in **a** and **b**. **c**, A trace of the centroid of the filament image in **a**. The trace starts at the filled square and ends at the open square. The first revolution is shown in the thick line.

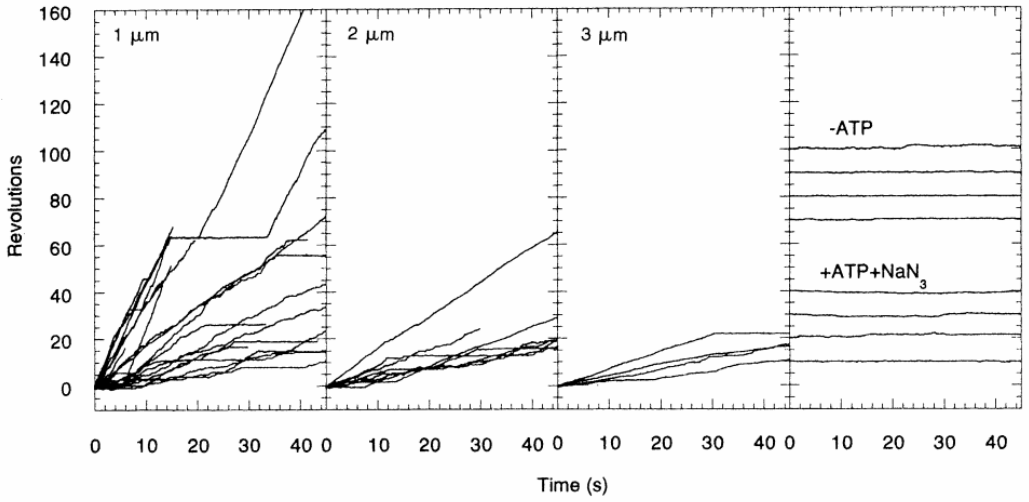

Figure 3 Time course of the rotation of the γ-subunit; each line represents one filament. The ordinate represents the number of anticlockwise revolutions. Rotating filaments, all in the presence of 2 mM ATP, are classified into three groups according to their length ('1 μm' indicates 0.5–1.4 μm; '2 μm', 1.5–2.4 μm; '3 μm', 2.5–3.4 μm). Only those filaments that rotated around one end are shown, for which the rotating angles were conveniently estimated by centroid analysis as in Fig. 2c. The angular resolution in these plots is estimated to be ~20°, or worse in some cases, because the filament was not always straight and part of the filament occasionally went out of focus. '−ATP', without ATP, '+ATP + NaN_3', in the presence of 2 mM ATP and 10 mM NaN_3; for these control experiments, those filaments that moved most are selected and shown.

Observation of rotation. Actin filaments were observed under an epifluorescence microscope (Diaphot TMD, Nikon) with excitation and emission wavelengths at 546 nm and 560–620 nm, respectively. Images were taken with a CCD camera (Dage MTI) attached to an image intensifier (KS-1381, Videoscope), recorded on an 8-mm video tape, and analysed with a digital image processor (DIPS-C2000, Hamamatsu Photonics)[2,23]. The frictional torque for the propeller rotation is given[24], in the simplest approximation, by $(\pi/3)\omega\eta L^3/[\ln(L/2r) - 0.447]$, where ω is the angular velocity, η (10^{-3} N s m^{-2}) the viscosity of the medium, L the length of actin filament, and r (5 nm) the radius of the filament. For the rotation around one end of the filament, the torque is four times the above value. These values are actually underestimated, because the viscous drag near the glass surface is higher (up to ~3-fold[24] if all of the filament lies at a height of (5 + 8) nm from the glass surface, 5 nm being the filament radius and 8 nm the height[8] of $\alpha_3\beta_3$) and because possible contact with the surface would produce additional friction.

Methods

Materials. The mutant (α-C193S, γ-S107C) $\alpha_3\beta_3\gamma$ subcomplex of thermophilic *Bacillus* PS3 was purified as described[21]. The subcomplex was treated with a 2–10 molar excess of 6-{*N'*-[2-(*N*-maleimido)ethyl]-*N*-piperazinylamido}hexyl-D-biotinamide (biotin-$PEAC_5$-maleimide, Dojindo) in 20 mM 3-[*N*-morpholino]propanesulphonic acid-KOH (MOPS-KOH, pH 7.0) and 100 mM KCl for 6 h on ice. Specific biotinylation of the γ-subunit was confirmed by western blotting with horseradish peroxidase avidin D (Vector Labs). Catalytic activities were measured at 25 °C at pH 7.0 in the presence of 50 mM KCl; the mutant subcomplex hydrolysed 52 ATP molecules per second, the wild-type subcomplex 52 ATP s^{-1}, and the native F_1-ATPase 39 ATP s^{-1}. Rabbit skeletal actin (30 μM) was incubated with 150 μM biotin-$PEAC_5$-maleimide in 100 mM KCl, 1 mM $MgCl_2$, 10 mM MOPS-KOH (pH 7.0) and 0.3 mM NaN_3 at room temperature for 2 h. The actin was depolymerized in 2 mM MOPS-KOH (pH 7.0), 0.2 mM $CaCl_2$ and 2 mM ATP. Residual biotin was removed on a Sephadex G-25 column. Biotinylated actin (5 μM) was polymerized in 10 mM 2-(cyclohexylamino)ethanesulphonic acid-KOH (pH 8.8), 100 mM KCl, 1 mM $MgCl_2$ and 5 μM phalloidin–tetramethylrhodamine B isothiocyanate conjugate (Fluka) overnight at 4 °C, and crosslinked with 500 μM disuccinimidyl suberate (Pierce) at room temperature for 2 h. The reaction was quenched with 50 mM Tris-HCl (pH 8.8).

Immobilization of proteins. A flow cell for microscopic observation was constructed from a bottom coverslip (24 × 36 mm^2; Matsunami) coated with nitrocellulose and a top coverslip (18 × 18 mm^2), separated by two greased strips of Parafilm cover sheet. 0.6–1.2 μM of horseradish peroxidase-conjugated Ni-NTA (Qiagen) was introduced into the flow cell and allowed to adhere to the glass surface for 2 min. The cell was washed with buffer A (10 mg ml^{-1} BSA, 10 mM MOPS-KOH (pH 7.0), 50 mM KCl, 4 mM $MgCl_2$). Infusion and washing were repeated as follows: infusion of 10–100 nM biotinylated $\alpha_3\beta_3\gamma$ subcomplex in buffer A (5 min), washing with buffer A, infusion of 180 nM streptavidin (Sigma) in buffer A (2 min), washing with buffer A, and infusion of 100 nM biotinylated fluorescent actin filaments in buffer A (5–15 min). The last wash was carried out with 0.5% 2-mercaptoethanol and an oxygen-scavenger system[22] in buffer A containing, where indicated, 2 mM ATP or 10 mM NaN_3. Observation started within 1 min of the beginning of the last washing. The actin filaments did not bind to the glass plate without the biotinylated subcomplexes. Also, the binding was dependent on streptavidin. In a control experiment, His-tagged subcomplexes fluorescently labelled at γ-Cys107 were fixed on a Ni-NTA surface and extensively washed with buffer A; subsequent washings with buffer A containing 50 mM imidazole (pH 7.4) removed >85% of the fluorescence. These results ensure that the actin filaments were attached to the biotinylated $\alpha_3\beta_3\gamma$ subcomplexes which were fixed to the glass surface through the histidine tags.

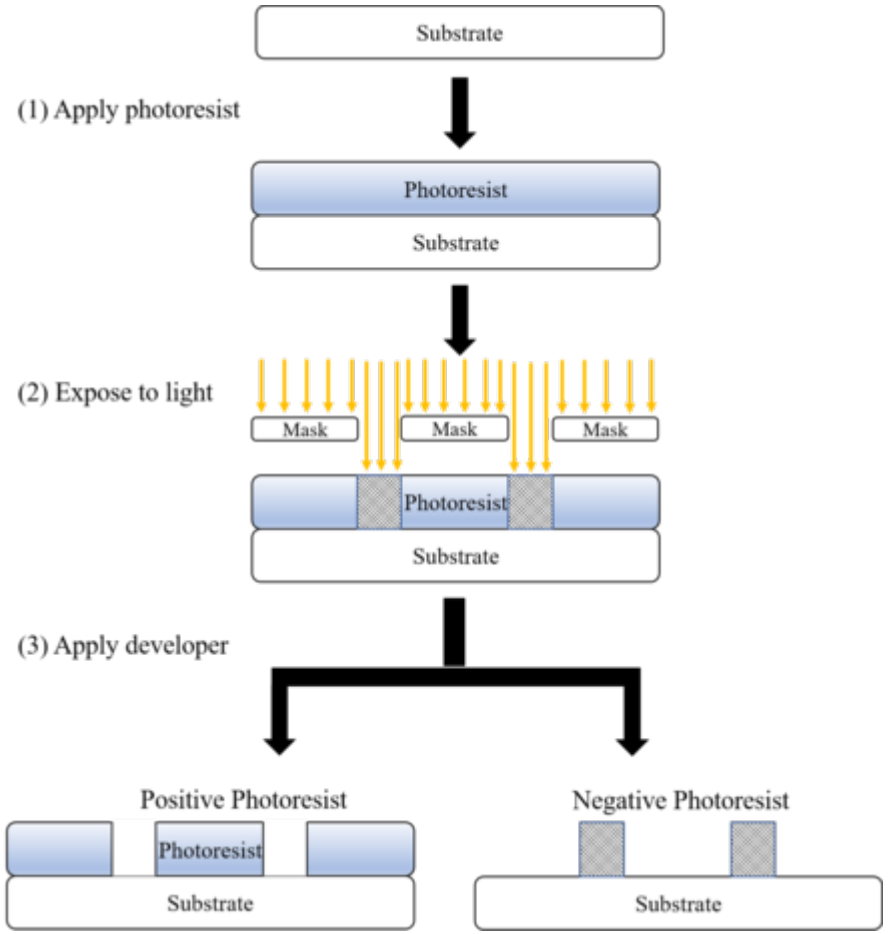

Positive Photoresist

A *positive resist* is a type of photoresist in which the portion of the photoresist that is exposed to light becomes soluble to the photoresist developer. The unexposed portion of the photoresist remains insoluble to the photoresist developer.

Negative Photoresist

A *negative photoresist* is a type of photoresist in which the portion of the photoresist that is exposed to light becomes insoluble to the photoresist developer. The unexposed portion of the photoresist is dissolved by the photoresist developer.

Litografia elettronica per fare i supporti di Ni

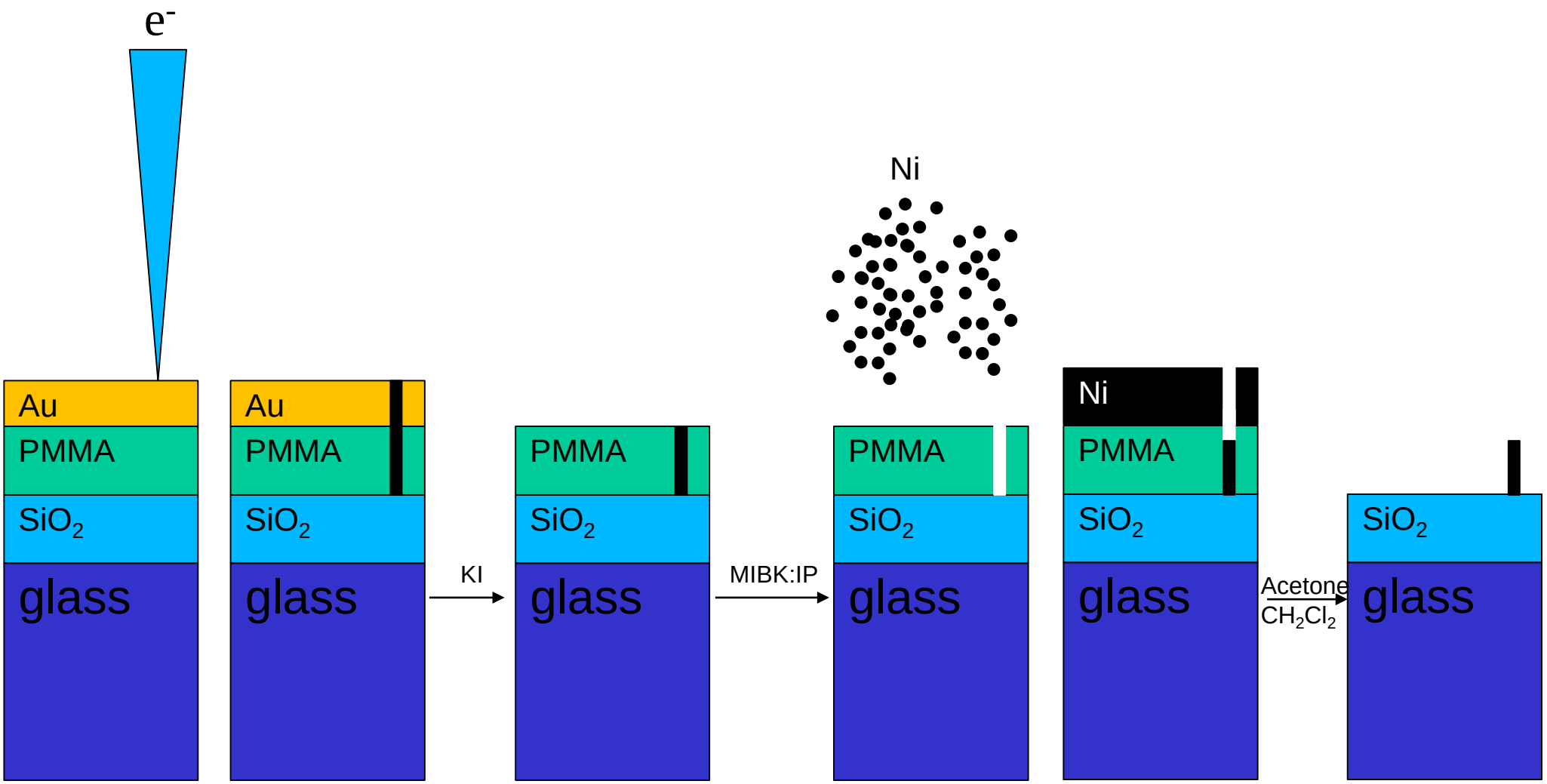

PMMA è un photoresist positivo
Il fascio elettronico rompe localmente il PMMA, rendendolo solubile in MIBK:IP (che non scioglie il PMMA)
Acetone e cloruro di metilene sciolgono il PMMA.